Published in final edited form as:
Spine J. 2010 December ; 10(12): 1089–1097. doi:10.1016/j.spinee.2010.09.014.

Structured Co-culture of Stem Cells and Disc Cells Prevent Degeneration in a Rat Model

Aliza A. Allon[1], **Nicolas Aurouer**[1,2], **Bryan B. Yoo**[1], **Ellen C. Liebenberg**[1], **Zorica Buser**[1], and **Jeffrey C. Lotz**[1]

[1] Department of Orthopaedic Surgery, University of California San Francisco, CA, USA

[2] Spinal Unit, Bordeaux Hospital University Center, Néant, France

Introduction

Stem cells are a potentially valuable component of intervertebral disc tissue engineering strategies that may, in the future, provide a minimally invasive low back pain treatment. Mesenchymal stem cells (MSCs) are being considered for this purpose, however previous studies demonstrate the powerful influence the local milieu has on MSC differentiation and matrix synthesis. Given the challenging environment within degenerate discs, in vivo studies are needed to test the plausibility of therapeutic efficacy as well as safety [1–5].

Rodents are desirable models for disc repair studies due to their low cost, ease of care, and fast healing times [6]. Tail discs are advantageous because of easy surgical access that allows multiple discs to be treated within each animal [7]. Additionally, rodent disc mechanics and innervation patterns are similar to those of humans, which is important for replicating relevant pathological processes [8–9].

Disc degeneration is triggered by an annular stab (where a surgical incision is made in the annulus fibrosus – depressurizing the disc) in various animal models including the rat [10–11], rabbit [12–16,23], dog [17], sheep [18–19], goat [20], and pig [21–22]. The annular stab technique induces morphological features pathognomonic of age-related degeneration in humans including: radial and concentric annular tears, endplate sclerosis, changes in cellularity and matrix composition, and pro-inflammatory cytokine production [24–25]. The annular incision can be preformed with nucleotomy that has the added benefit of eliminating the contribution of notochordal cells to the healing process, thereby increasing the clinical relevance [26–28].

The acute stage of disc injury is characterized by inflammatory cytokine production, ischemia, decreased pH, and alterated tissue stress [29–31]. These features challenge the retention and survival of cells introduced to orchestrate disc healing. Previous attempts at injecting MSCs into the disc have had varied results with limited therapeutic efficacy [34–38]. This is likely due to poor survival, undesirable differentiation, and ineffectual matrix synthesis [37–39]. Similarly, allograft nucleus pulposus cells (NPCs) have limited synthetic activity [40–42]. Combinations of cells and scaffolds have also been implanted in animals,

Corresponding author: Jeffrey C. Lotz, UCSF Orthopaedic Bioengineering Laboratory, 533 Parnassus Ave, U454, San Francisco, CA 94143-0514, p. 415.476.7881, f. 415.476.1128, lotzj@orthosurg.ucsf.edu.

but have yet to show long term benefits [42–44]. Consequently, though progress is being made with cell-based therapies, there are still many obstacles to clinical success in the spine due to the harsh degenerate disc environment where inflammation, ischemia, and pressure inhibit the cells' abilities to mount a therapeutic response [2,10,38–40].

In order to address these issues, we have developed a novel spherical bi-laminar cell pellet (BCP) where MSCs form an inner-sphere enclosed within a shell of NPCs with a 75:25 cell ratio respectively. In a simulated degenerate disc environment *in vitro*, BCPs have a 48% increase in proteoglycan-synthesis as compared to single cell-type controls [2]. The current study tests the BCP's potential as a therapeutic in the rat tail model with the objective to compare the therapeutic efficacy of BCPs to suspensions of either MSCs or NPCs. In all groups, fibrin sealant was used as a delivery vehicle into denucleated discs.

Methods

Rat selection, Anesthesia, and Surgical Procedure

Sixty 6-month old male Sprague Dawley Rats (250 grams) were used with IACUC approval. Prior to surgery, each animal was anesthetized (by inhaling isofluorane) and medicated with buprenorphine (0.01 mg/kg body weight). While under anesthesia, the animal's paw pinch response and respiration pattern were monitored every 5 min.

After placing the animal under general anesthesia, the tail was cleaned with a surgical scrub and an occlusion cuff was placed proximally. The cuff limited tail blood flow allowing the discs to be easily visualized while minimizing blood loss. A longitudinal incision (approximately 3cm long) was made to expose the three most cranial tail discs. Lateral stabs were performed in each disc using a number 11 blade. The nucleus pulposus was removed using a curette and the desired treatment was inserted into the nucleus cavity. The annulus was then closed with two 5.0 non-resorbable nylon sutures. The occlusion cuff was then removed. The cuff was on the tail for no longer than 15 minutes. Finally, the tail skin was closed using resorbable sutures. Following the procedure, rats were allowed unrestricted activity and monitored for signs of pain or infection. Buprenorphine (0.01–0.02 mg/kg, SQ) was administered as needed for pain.

After the appropriate treatment duration, the rats were euthanized by carbon dioxide asphyxiation followed by bilateral thoracotomy and the discs were harvested for analysis. Two time points were selected for the study: 2 weeks to assess the acute post-injury state; and 5 weeks to assess the chronic responses. These time points were also selected based on the predicted persistence of fibrin sealant, which is present at 2 weeks but degraded after 5 weeks.

Treatment groups

Sixty rats were assigned to one of six groups assessed at the 2 time points: stab and denucleation only (Stab group), fibrin-sealant (FS) only (Fibrin group), MSCs suspension in FS (MSC group), NPCs suspension in FS (NPC group), NPCs and MSCs suspension in FS (Mix group), BCP with FS (BCP group: Figure 1). Three discs were treated in each rat, giving 15 discs per group per time point. The Stab group serves as a positive control to assess the unobstructed acute inflammatory cycle. The Fibrin group serves as a negative control for cell treatment, while the other groups serve to characterize the treatment efficacy.

Cells and fibrin

MSCs were commercially obtained (Lonza, Switzerland) and expanded to the 7^{th} passage in growth media (DMEM low glucose, 1% antibiotic/antimycotic, and 10% FBS) at 37°C with

5% CO_2. NPCs were isolated from adult bovine tails and expanded to the 4th passage. Surgical grade FS was obtained from commercial sources (TISSEEL, Baxter, IL).

In each case of cell treatment, a total of 250,000 cells were inserted into the nucleus space with 4uL of FS. In the cases of cell suspensions, the cells were homogeneously suspended in the FS prior to insertion. In the case of BCP, the BCP was formed 7 days prior to insertion in order for it to become spherical using 75% MSC on the inside and 25% NPC on the outside with a total of 250,000 cells. The BCP was first placed in the disc space and then covered with 4uL of FS (Figure 2).

Histology, Disc height, and Disc Grade

For each group, five disc samples from both time points were processed for decalcified, paraffin-embedded histology and stained with Safranin-O. To identify human cells, human specific antibody Lamp 1&2 was immunolocalized within each section (Abcam, MA).

Disc height measurements were taken from growth plate to growth plate on histologic samples (n=5 per group per time point). For each image, the height was determined by an average of three measurements made in three areas of the disc space: on the left side, center, and the right side. Disc grade was assessed in a blinded fashion using a scheme based on morphology and cellularity (Table 1).

ELISA, DMMB, and PCR

Five of the disc samples per group from both time points were evaluated for cytokine content. The entire discs were separated from the vertebrae, digested using TPER buffer (Pierce, IL), and quantified using enzyme linked immune-sorbent assay (ELISA) for rat IL-1b, IL-4, and TNF-a (R&D Systems, MN) (n=5 per group per time point).

Digested samples used for ELISA were also assayed with a dimethylmethylene blue (DMMB) assay to quantify GAG content (n=5 per group per time point). A standard curve was made with chondroitin sulfate isolated from bovine trachea (Sigma, MO). Absorption was measured at 525nm using a spectrophotometer.

Finally, five discs were allocated for real time quantitative PCR to identify the presence of human MSC and bovine NPC (n=5 per group per time point). The entire discs were separated from the vertebrae and RNA was extracted using a QIAshredder Fibrous Tissue mini kit (Qiagen, Germany). The RNA was reverse transcribed using iScript (Bio-Rad Laboratories, CA). The samples were analyzed using species specific primers (Table 2) for human and bovine housekeeping genes and quantified using iQ Sybr Green Supermix (Bio-Rad Laboratories, CA). The cell retention rate was defined as 100% for the sample if the threshold cycle value was above 35 for the housekeeping gene of interest. The overall rate was then determined by averaging the five samples.

All statistical analyses were preformed using JMP statistical software (Version 5.0). Standard analysis of variance procedures were performed to compare group means and to estimate the effect of the specimen group variables. The Tukey-Kramer test was used to determine pair-wise statistical differences.

Results

Disc Height

At the 2 week time point, the NPC group had a disc height from 25% to 44.7% higher than all other groups except the Fibrin group ($p<0.05$). By 5 weeks, the BCP group had a disc height from 29% to 118% greater than all groups except those of the NPC and MSC group

($p<0.05$) (Table 3). Disc heights decreased with time for all groups except for the BCP group where heights increased by an average of 3.6 mm (8.7 %) (Figure 3).

Disc Grade

At the 2 week time point, there were no significant differences in disc grade between the groups (Table 4). However, there was a trend of the NPC, Mix, and BCP groups having better disc quality than the MSC, Fibrin, and Stab groups. At the 5 week time point, the histologic score for the BCP group was significantly improved relative to the other groups (2.14 ± 0.29; $p<0.05$). In addition, the BCP group was the only group to improve its disc grade between the 2 and 5 weeks time points.

Histology

Normal, untreated discs were used as the basis of comparison (Figure 4). The treated groups were examined for the presence of native notochordal cells which appeared not to be present due to the nucleotomy. As early as the 2 week time point, the Stab group displayed a collapse in disc height and disruption to the endplate and growth plate (Figure 5A). In all other treatment groups, the disc height was well preserved though there was no apparent proteoglycan staining or cellularity in the nucleus. In the BCP treated group, the pellet was apparent in the nucleus and a small amount of proteoglycan has begun to deposit (Figure 5F).

At the 5 week time point, all the groups except the BCP experienced severe disruption of the endplate, growth plate, and annulus in addition the disc height was diminished and there was significant loss of cellularity (Figure 6A–E). In the BCP-treated discs, disc morphology was better preserved (Figure 6F). The disc height was conserved as was the integrity of the annulus, endplate, and growth plate. The BCP group was the only treatment to demonstrate any proteoglycan staining in the disc space.

Maintenance of BCP structure and retention within the disc was confirmed at 5 weeks using a human specific antibody (LAMP 1&2) (Figure 7E). Furthermore, proteoglycan matrix localized within the nucleus (Figure 7D) co-localized with human cells within the BCP (Figure 7E). In some cases, the BCP, centralized within the nucleus, appeared to begin to integrate with the adjacent tissue (Figure 7F).

DMMB, ELISA, and PCR

There were no statistically-significant differences in DMMB values between any group at any time point. The ELISAs for IL-4 and TNF-a were below detection limits. There was a downward trend between 2wk and 5wks for IL-1b, but this did not reach statistical significance (Figure 8).

At the 2 week time point, the MSC had a 60–80% lower cell retention rate than the Mix and BCP groups ($p<0.05$; Table 5). At 5 weeks, MSC had a 20–40% lower cell retention than the Mix and BCP group though it was not significant. The NPC group had similar cell retention rates as the Mix and BCP groups for both time points.

Discussion

The goal of this study was to test whether in vitro benefits of BCPs translate to the in vivo setting. We used several criteria to evaluate the treatment's performance including quantitative measures of disc height and quality, qualitative histologic evaluation, and measurements of cytokines, proteoglycan, and the retention of implanted cells. Our results

suggest that the BCP offers advantages over single cell type approaches and cell-suspension approaches.

At 2 weeks after surgery, the disc height was well maintained for all groups except the Stab discs. Yet, there was no apparent presence of new matrix within the nucleus for any of the discs with the exception of the BCP group. Therefore, we believe that early disc height preservation is primarily due to the mass effect of the FS as demonstrated by the fact that the Fibrin group had among the best disc heights. Similarly, it is likely that overall disc quality and morphology was also preserved early on at least in part by the FS.

By 5 weeks, both the Stab and Fibrin groups had collapsed discs and the Mix group had the third lowest disc height. This is an indication that FS had resorbed and was no longer supporting disc height maintenance. Rather, nuclear volume was being maintained by the cellular content in the case of the top three groups of MSC, NPC, and BCP. Disc height preservation due to MSC injection has been observed in other in vivo studies [46–49]. The BCP group was the only group to have a mean increase in disc height and it was also the only group to show any proteoglycan staining and high cellularity in the disc space. This suggests a synthetic activity by BCP group that may be responsible for disc height preservation.

The ELISA for IL-1beta did detect varying levels of cytokine at the 2 week time point which dropped overall by 5 weeks. This is an indication that the inflammatory response was associated with the surgical procedure and not with any specific treatment (e.g. as a reaction to a xenograph). The levels of IL-4 and TNF-a were below detection limits.

While the BCP group did show proteoglycan staining in the disc space that appeared to increase over time, the DMMB measurements were not significantly different between groups. Longer time points may be required for sufficient new matrix to accumulate to enable detection of protein differences beyond animal to animal variability.

At the 2 week time point, MSC were significantly less well retained than the BCP and Mix group. Similar findings of low MSC retention were reported in other in vivo studies [35,50]. This is in contrast to the NPC which were well retained in our study as well as in others [14,41]. This difference in retention is likely due to MSC susceptibility to adverse environmental factors. In particular, hypoxia and nutrient deprivation (i.e. ischemia) are well known impediments for cell-based tissue engineering constructs. Specifically, prolonged ischemia is known to lead to stem cell death [52] and potentiate inflammation [53]. Taken together, these observations suggest that a patient's degenerate/painful disc environment would not be conducive to cell-based repair strategies using undifferentiated MSCs. However, when the MSC were combined with NPC in the Mix and BCP groups performance improved, as previously shown in vitro [2], and may be an indication of a therapeutically relevant result.

Our results are limited by several aspects of the chosen animal model [10–11]. Annular incision and nucleotomy trigger rapid degeneration that isn't physiologically equivalent to human disc degeneration that occurs slowly over a lifetime [26–28]. In addition, tail discs do not have the same load bearing profile as those of the human lumbar spine. Most importantly, the ischemic stress in rat discs isn't comparable to that in much larger human discs [29–31]. Consequently, future studies of BCPs in larger animal models that more closely mimic the human situation are warranted.

Despite these limitations, our data suggest improved BCP performance in vivo that parallel beneficial behaviors previously reported for in vitro models. Resilience of BCP to pressure, ischemia, and inflammation provide a functional advantage that appears to translate into

clinically-relevant benefits as demonstrated by improved disc height, disc grade, the retention of implanted cells, and the synthesis of new matrix in the disc space.

Acknowledgments

This work was supported by NIH AR052712 to JCL.

References

1. Yoo JU, Barthels TS, Nishimura K, et al. The chondrogenic potential of human bone-marrow derived mesenchymal progenitor cells. J Bone Joint Surg Am 1998;80A(12):1745–1757. [PubMed: 9875932]
2. Allon AA, Butcher K, Schneider RA, Lotz JC. BCP in disc mimetic environment. 2010 in submission.
3. Singh K, Masuda K, ANHS. Animal models for human disc degeneration. Spine J 2005;5(6 Suppl): 267S–279S. [PubMed: 16291123]
4. An HS, Masuda K. Relevance of in vitro and in vivo models for intervertebral disc degeneration. J Bone Joint Surg Am 2006;88 (Suppl 2):88–94. [PubMed: 16595451]
5. Lotz JC. Animal models of intervertebral disc degeneration: lessons learned. Spine (Phila Pa 1976) 2004;29(23):2742–50. [PubMed: 15564923]
6. Schimandle JH, Boden SD. Spine update. Animal use in spinal research. Spine (Phila Pa 1976) 1994;19(21):2474–7. [PubMed: 7846605]
7. Elliott DM, Sarver JJ. Young investigator award winner: validation of the mouse and rat disc as mechanical models of the human lumbar disc. Spine (Phila Pa 1976) 2004;29(7):713–22. [PubMed: 15087791]
8. Hunter CJ, Matyas JR, Duncan NA. Cytomorphology of notochordal and chondrocytic cells from the nucleus pulposus: a species comparison. J Anat 2004;205(5):357–62. [PubMed: 15575884]
9. Aoki Y, Ohtori S, Ino H, et al. Disc inflammation potentially promotes axonal regeneration of dorsal root ganglion neurons innervating lumbar intervertebral disc in rats. Spine (Phila Pa 1976) 2004;29(23):2621–6. [PubMed: 15564910]
10. Ulrich JA, Liebenberg EC, Thuillier DU, Lotz JC. ISSLS prize winner: repeated disc injury causes persistent inflammation. Spine (Phila Pa 1976) 2007;32(25):2812–9. [PubMed: 18246002]
11. Rousseau MA, Ulrich JA, Bass EC, Rodriguez AG, Liu JJ, Lotz JC. Stab incision for inducing intervertebral disc degeneration in the rat. Spine (Phila Pa 1976) 2007;32(1):17–24. [PubMed: 17202887]
12. Lipson SJ, Muir H. 1980 Volvo award in basic science. Proteoglycans in experimental intervertebral disc degeneration. Spine (Phila Pa 1976) 1981;6(3):194–210. [PubMed: 7268542]
13. Takaishi H, Nemoto O, Shiota M, et al. Type-II collagen gene expression is transiently upregulated in experimentally induced degeneration of rabbit intervertebral disc. J Orthop Res 1997;15(4): 528–38. [PubMed: 9379262]
14. Nomura T, Mochida J, Okuma M, Nishimura K, Sakabe K. Nucleus pulposus allograft retards intervertebral disc degeneration. Clin Orthop Relat Res 2001;(389):94–101. [PubMed: 11501830]
15. Anderson DG, Izzo MW, Hall DJ, et al. Comparative gene expression profiling of normal and degenerative discs: analysis of a rabbit annular laceration model. Spine (Phila Pa 1976) 2002;27(12):1291–6. [PubMed: 12065976]
16. Masuda K, Aota Y, Muehleman C, et al. A novel rabbit model of mild, reproducible disc degeneration by an anulus needle puncture: correlation between the degree of disc injury and radiological and histological appearances of disc degeneration. Spine (Phila Pa 1976) 2005;30(1): 5–14. [PubMed: 15626974]
17. Hampton D, Laros G, McCarron R, Franks D. Healing potential of the anulus fibrosus. Spine (Phila Pa 1976) 1989;14(4):398–401. [PubMed: 2718042]
18. Osti OL, Vernon-Roberts B, Fraser RD. 1990 Volvo Award in experimental studies. Anulus tears and intervertebral disc degeneration. An experimental study using an animal model. Spine (Phila Pa 1976) 1990;15(8):762–7. [PubMed: 2237626]

19. Moore RJ, Vernon-Roberts B, Osti OL, Fraser RD. Remodeling of vertebral bone after outer anular injury in sheep. Spine (Phila Pa 1976) 1996;21(8):936–40. [PubMed: 8726196]
20. Ethier DB, Cain JE, Yaszemski MJ, et al. The influence of anulotomy selection on disc competence. A radiographic, biomechanical, and histologic analysis. Spine (Phila Pa 1976) 1994;19(18):2071–6. [PubMed: 7825048]
21. Kaapa E, Holm S, Han X, Takala T, Kovanen V, Vanharanta H. Collagens in the injured porcine intervertebral disc. J OrthopRes 1994;12(1):93–102.
22. Kanerva A, Kommonen B, Gronblad M, et al. Inflammatory cells in experimental intervertebral disc injury. Spine (Phila Pa 1976) 1997;22(23):2711–5. [PubMed: 9431603]
23. Sobajima S, Kompel JF, Kim JS, et al. A slowly progressive and reproducible animal model of intervertebral disc degeneration characterized by MRI, X-ray, and histology. Spine (Phila Pa 1976) 2005;30(1):15–24. [PubMed: 15626975]
24. Boos N, Weissbach S, Rohrbach H, Weiler C, Spratt KF, Nerlich AG. Classification of age-related changes in lumbar intervertebral discs: 2002 Volvo Award in basic science. Spine (Phila Pa 1976) 2002;27(23):2631–44. [PubMed: 12461389]
25. Sobajima S, Shimer AL, Chadderdon RC, et al. Quantitative analysis of gene expression in a rabbit model of intervertebral disc degeneration by real-time polymerase chain reaction. Spine J 2005;5(1):14–23. [PubMed: 15653081]
26. Hasegawa K, Turner CH, Chen J, Burr DB. Effect of disc lesion on microdamage accumulation in lumbar vertebrae under cyclic compression loading. Clin Orthop Relat Res 1995;(311):190–8. [PubMed: 7634575]
27. Nishimura K, Mochida J. Percutaneous reinsertion of the nucleus pulposus. An experimental study. Spine (Phila Pa 1976) 1998;23(14):1531–8. discussion 1539. [PubMed: 9682309]
28. Hiyama A, Mochida J, Iwashina J, et al. Transplantation of mesenchymal stem cells in a canine disc degeneration model. J Orthop Res 2008;26(5):589–600. [PubMed: 18203202]
29. An HS, Masuda K. Relevance of in vitro and in vivo models for intervertebral disc degeneration. J Bone Joint Surg Am 2006;88 (Suppl 2):88–94. [PubMed: 16595451]
30. Lotz JC, Staples A, Walsh A, Hsieh AH. Mechanobiology in intervertebral disc degeneration and regeneration. Conf Proc IEEE Eng Med Biol Soc 2004;7:5459. [PubMed: 17271585]
31. Lotz JC, Ulrich JA. Innervation, inflammation, and hypermobility may characterize pathologic disc degeneration: review of animal model data. J Bone Joint Surg Am 2006;88 (Suppl 2):76–82. [PubMed: 16595449]
32. Sheikh H, Zakharian K, et al. In vivo intervertebral disc regeneration using stem cell-derived chondroprogenitors. J Neurosurg Spine 2009;10(3):265–72. [PubMed: 19320588]
33. Hiyama A, Mochida J, Sakai D. Stem cell applications in intervertebral disc repair. Cell Mol Biol 2008;54(1):24–32. [PubMed: 18954548]
34. Saldanha KJ, Piper SL, et al. Magnetic resonance imaging of iron oxide labeled stem cells: application to tissue engineering based regeneration of the intervertebral disc. Eur Cell Mater 2008;16:17–25. [PubMed: 18677684]
35. Sakai D, Mochida J, et al. Differentiation of mesenchymal stem cells transplanted to a rabbit degenerative disc model: potential and limitations for stem cell therapy in disc regeneration. Spine (Phila Pa 1976) 2005;30(21):2379–87. [PubMed: 16261113]
36. Risbud MV, Shapiro IM, et al. Stem cell regeneration of the nucleus pulposus. Spine J 2004;4(6 Suppl):348S–353S. [PubMed: 15541688]
37. Bibby SR, Jones DA, et al. Metabolism of the intervertebral disc: effects of low levels of oxygen, glucose, and pH on rates of energy metabolism of bovine nucleus pulposus cells. Spine (Phila Pa 1976) 2005;30(5):487–96. [PubMed: 15738779]
38. Horner HA, Urban JP. Effect of nutrient supply on the viability of cells from the nucleus pulposus of the intervertebral disc. Spine (Phila Pa 1976) 2001;26(23):2543–9. [PubMed: 11725234]
39. Lotz JC, Chin JR. Intervertebral disc cell death is dependent on the magnitude and duration of spinal loading. Spine (Phila Pa 1976) 2000;25(12):1477–83. [PubMed: 10851095]
40. Gruber HE, Ingram JA, et al. Increased cell senescence is associated with decreased cell proliferation in vivo in the degenerating human annulus. Spine J 2009;9(3):210–5. [PubMed: 18440281]

41. Gorensek M, Jaksimovic C, et al. Nucleus pulposus repair with cultured autologous elastic cartilage derived chondrocytes. Cell Mol Biol Lett 2004;9(2):363–73. [PubMed: 15213815]

42. Chou, Al; Akintoye, SO.; Nicoll, SB. Photo-crosslinked alginate hydrogels support enhanced matrix accumulation by nucleus pulposus cells in vivo. Osteoarthritis Cartilage 2009;17(10):1377–84. [PubMed: 19427928]

43. Nesti LJ, Li WJ, et al. Intervertebral disc tissue engineering using a novel hyaluronic acid-nonfibrous scaffold amalgam. Tissue Eng Part A 2008;14(9):1527–37. [PubMed: 18707229]

44. Yang X, Li X. Nucleus pulposus tissue engineering: a brief review. Eur Spine J. 2009 Jul 15; Epub.

45. Allon AA, Butcher K, et al. Bilaminar co-culture. 2010 in submission.

46. Jeong JH, Jin ES, Min JK, et al. Human mesenchymal stem cells implantation into the degenerated coccygeal disc of the rat. Cytotechnology 2009;59(1):55–64. [PubMed: 19363673]

47. Chen WH, Liu HY, Lo WC, et al. Intervertebral disc regeneration in an ex vivo culture system using mesenchymal stem cells and platelet-rich plasma. Biomaterials 2009;30(29):5523–33. [PubMed: 19646749]

48. Sakai D, Mochida J, Iwashina T, et al. Regenerative effects of transplanting mesenchymal stem cells embedded in atelocollagen to the degenerated intervertebral disc. Biomaterials 2006;27(3): 335–45. [PubMed: 16112726]

49. Crevensten G, Walsh AJ, Ananthakrishnana D, et al. Intervertebral disc cell therapy for regeneration: mesenchymal stem cell implantation in rat intervertebral discs. Ann Biomed Eng 2004;32(3):430–4. [PubMed: 15095817]

50. Sobajima S, Vadala G, Shimer A, Kim JS, Gilbertson LG, Kang JD. Feasability of a stem cell therapy for intervertebral disc degeneration. Spine J 2008;8(6):888–96. [PubMed: 18082460]

51. Potier E, Ferreira E, Meunier A, et al. Prolonged hypoxia concomitant with serum deprivation induces massive human mesenchymal stem cell death. Tissue Eng 2007;13(6):1325–31. [PubMed: 17518749]

52. Early SB, Hise K, Han JK, et al. Hypoxia stimulates inflammatory and fibrotic responses from nasal-polyp derived fibroblasts. Laryngoscope 2007;117(3):511–5. [PubMed: 17334314]

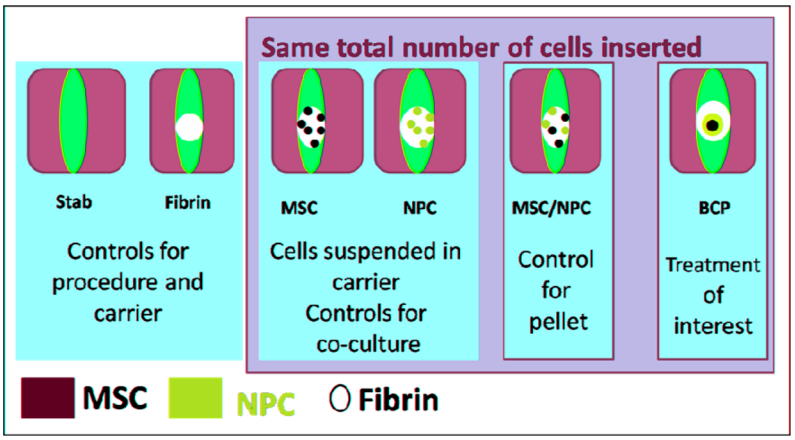

Figure 1.
The six treatment groups for 2 and 5 week time points.

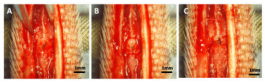

Figure 2.
A) The hole is made by de-nucleating the disc. B) The BCP is inserted into the disc space. C) The annulus is closed with sutures.

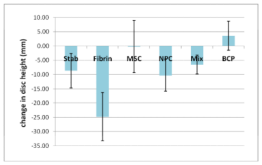

Figure 3.
Change in disc height from the 2 week time point to the 5 week time point in mm. The BCP group is the only group that is seeing an increase in disc height.

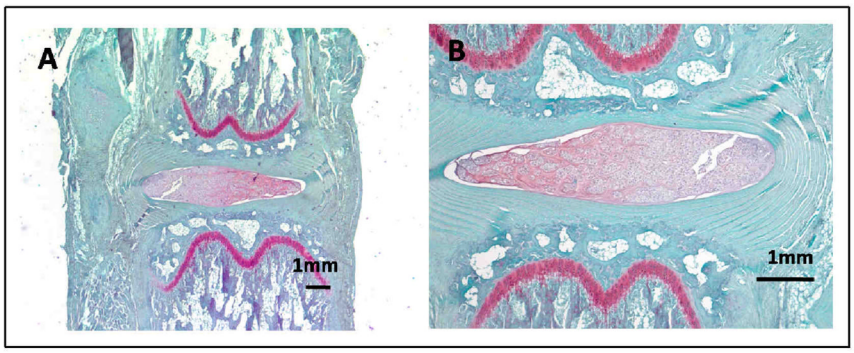

Figure 4.
Normal disc where the endplate and growth plates are intact. The nucleus pulposus is cellular and stains brightly red due to its high proteoglycan content. The annulus forms uninterrupted concentric lamellae.

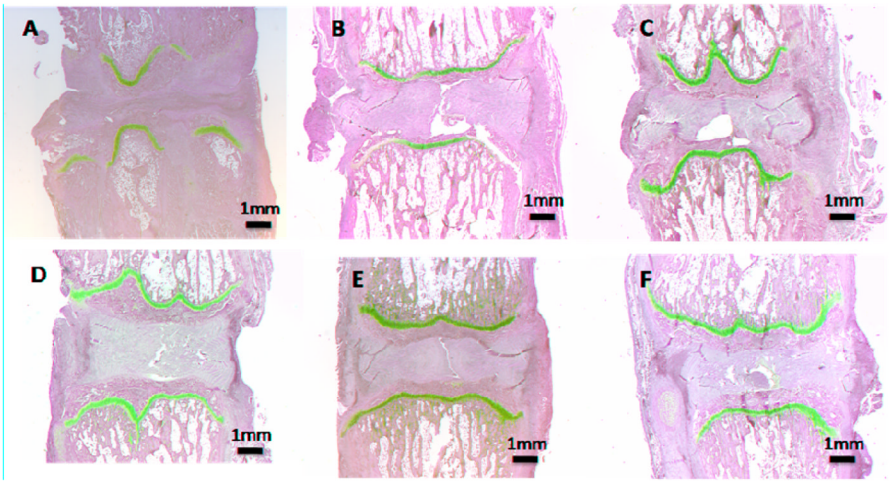

Figure 5.
Histologic images with Safranin-O staining for the 2 wk time point. A)Stab, B) Fibrin, C) MSC, D) NPC, E) Mix, F) BCP.

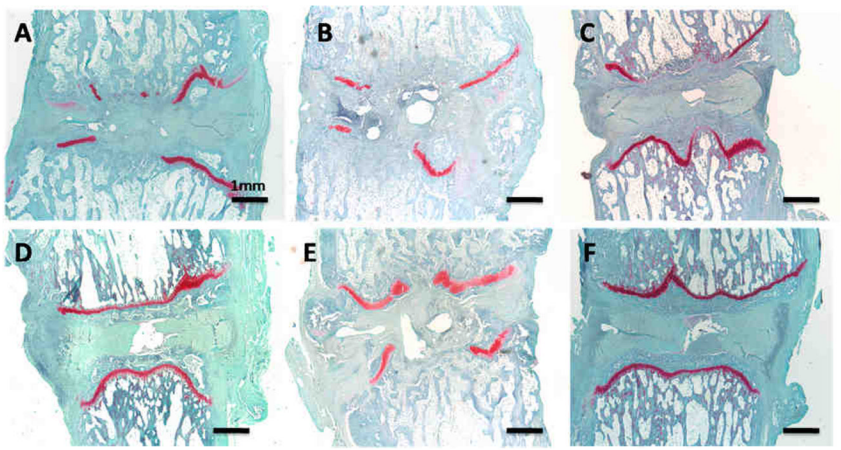

Figure 6.
Histologic images with Safranin-O staining for the 5 wk time point. A)Stab, B) Fibrin, C) MSC, D) NPC, E) Mix, F) BCP.

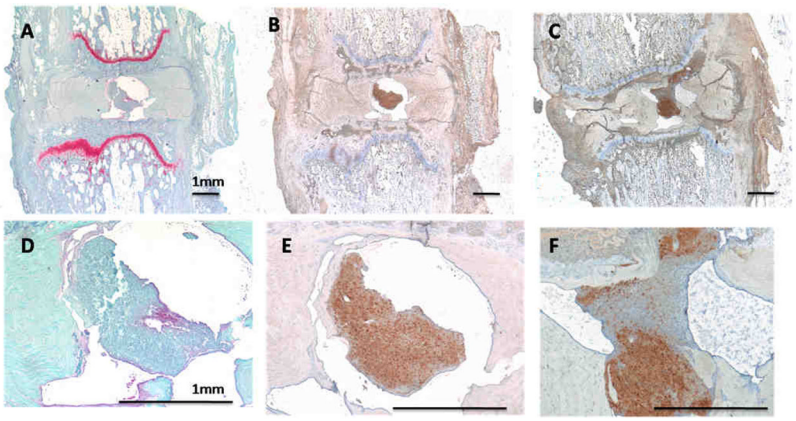

Figure 7.

A) 5wk BCP treated disc with Safranin-O staining. B) This is an adjacent section to image A but stained using immunohistochemistry for a human specific antibody (LAMP1&2) in brown. The brown stained cells represent cells that are from the BCP. Images D & E are magnified images of the nucleus space respectively of A & B. It is apparent in image D that the BCP has positive staining for proteoglycan. C) 5wk BCP treated disc stained with LAMP1&2 showing human cells in brown. F) Magnified version of C demonstrating that the BCP has begun integrating the host tissue and occupying the disc space.

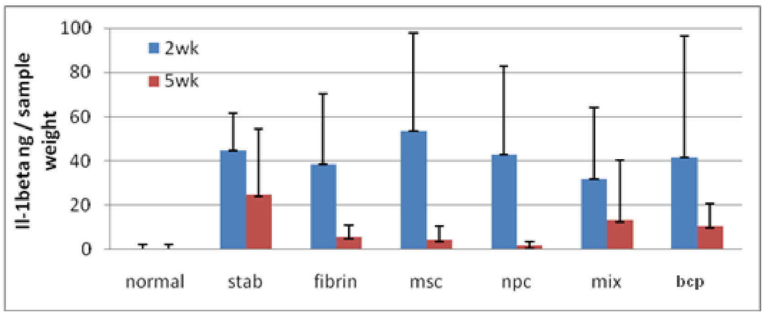

Figure 8.

Il-1beta ELISA. The data did not have any statistically significant differences among the groups. However, there was a downward trend between the 2nd and 5th week. This is an indication that there is no significant immunologic response to the xenograph.

Table 1

Disc grade was scored blindly according to the following categories. Each category was given a score from 1, for normal discs, to 5, for degenerative discs

Category	Score of 1 (normal)	Score of 5 (degenerative)
Annulus Fibrosus Grade	Normal pattern of fibrocartilage lamellae without ruptured fibers and without a serpentine appearance	Moderate/severe interruption
Border between the Annulus Fibrosus and the Nucleus Pulposus	Normal	Moderate/severe disruption
Cellularity of the Nucleus Pulposus grade	Normal Cellularity	Moderate/severe decrease in the number of cells
Matrix of the Nucleus Pulposus	Normal gelatinous appearance	Moderate/severe condensation of the matrix
Endplate grade	Normal continuous and undisrupted	Complete disruption
Growthplate grade	Normal continuous and undisrupted	Complete disruption
Disc height grade	Normal disc height	Complete collapse

Table 2

Species specific primers used for PCR

Gene	Forward	Reverse
Human GAPDH	5′-gga ggt gaa ggt cgg agt-3′	5′-gaa gat ggt gat ggg att tc-3′
Bovine B2M	5′-tgg gtt cca tcc acc cca ga-3′	5′-tca gcg tgg gac agc agg ta-3′

Table 3

Disc height measurements in mm arranged by group and time point. At the 2 week time point, NPC group is significantly higher than all groups except Fibrin ($p<0.05$). At the 5 week time point, BCP is significantly higher than all groups except NPC and MSC ($p<0.05$)

Group	2 week	5 week
Stab	40.08 ± 7.68	31.43 ± 4.47
Fibrin	47.62 ± 10.89	22.84 ± 6.00
MSC	45.84 ± 10.54	45.64 ± 7.71
NPC	58.00 ± 2.96 *	47.74 ± 8.32
Mix	45.22 ± 2.81	38.72 ± 3.78
BCP	46.30 ± 4.77	49.94 ± 5.38 *

Table 4

Disc grade determined from histologic images. Scores range from 1 (normal) to 5 (degenerative)

Group	2 week	5 week	Change between weeks 2–5
Stab	3.86 ± 1.62	5 ± 0	−1.14
Fibrin	3.24 ± 0.81	4.90 ± 0.16	−1.67
MSC	3.67 ± 0.98	3.71 ± 0.20	−0.05
NPC	2.71 ± 0.71	3.62 ± 0.41	−0.90
Mix	2.57 ± 0.88	3.90 ± 0.70	−1.33
BCP	2.86 ± 0.40	2.14 ± 0.29 *	0.71

Table 5

The retention of injected cells was measured using species specific primers with real time quantitative PCR. At 2 weeks, MSC had significantly lower retention rates than both the Mix and BCP groups ($p<0.05$)

Group	% retention of MSC		% retention of NPC	
	2 week	5 week	2 week	5 week
MSC	20*	40	NA	NA
NPC	NA	NA	60	60
Mix	100	80	60	60
BCP	80	60	80	60